Available online at www.sciencedirect.com
ScienceDirect
Catalysis Today 137 (2008) 439–445
CATALYSIS TODAY
www.elsevier.com/locate/cattod

Hydrogenation of aromatic compounds during gas oil hydrodewaxing I. Effect of ruthenium content and method of nickel catalyst preparation

Aleksandra Masalska

Wrocław University of Technology, Faculty of Chemistry, 7/9 Gdańska Street, 50-344 Wrocław, Poland

Available online 4 March 2008

Abstract

Ni-based (8 wt.% NiO) dewaxing catalysts for the hydroconversion of the hydroraffinate of oil fraction ($d_{20\ °C}$ = 0.845 g/cm^3; cloud point (CP) = −2 °C; aromatics = 25.8 wt.%; S = 25 ppm) were modified with Ru. The effect of Ru content (0.6, 0.75 and 0.9 wt.% of RuO_2) and the methods of Ni catalyst preparation were examined. The catalysts were characterised by N_2 sorption, TPR, ICP, XRD, SEM, XPS, H_2 chemisorption. Activity was tested in a continuous-flow system at 6 MPa (LHSV, 2.5 h^{-1}; H_2:CH, 350 N m^3/m^3). NiO and RuO_2 were found to exert a synergic effect on catalytic activity. The rise in RuO_2 content from 0.6 to 0.9 wt.% increased the HDA of HON from 23 to 65% at 240 °C and was parallelled by a drop in CP (by about 15 °C). The effect of Ru was found to depend on the method of Ni catalyst preparation.

Keywords: Dewaxing nickel catalyst; Ruthenium; Aromatics hydrogenation

1. Introduction

The study of emissions from diesel engines performed under the EPEFE programme [1] shows that the decrease in total aromatics content from 30 to 10% (m/m) reduces NO_X emission by 5 and 4% (light duty and heavy duty, respectively); the decrease in polyaromatics (di$^+$) from 9 to 1% reducing PM emissions by 6 and 4% (light duty and heavy duty, respectively). *World-wide Fuel Charter* suggests that total aromatics and polyaromatics content should not exceed 20 and 3% for category 3, and 15 and 2.0% for category 4 of diesel fuel, respectively.

The increasing demand for diesel fuel is covered, e.g., by the addition of components from destruction processes. This increases the content of aromatics (e.g., LCO from FCC contains up to 80 vol.% of aromatics [2]) and deteriorates the cold flow properties (e.g., diesel oil fraction from hydrocracking [3]). If dewaxing catalysts (used to improve the cold flow properties) of an increased hydrogenating function were used for the production of diesel oil, this would enable simultaneous conversion of *n*-paraffinic and aromatic hydrocarbons.

Ru is known to display not only a high hydrogenating activity (due to the low heat of H_2 adsorption [4]) but also a high thiotolerance compared to other monometallic noble metal catalysts, which is seemingly attributable to the low local density of unoccupied states at the Fermi level [5,6]. Some investigators have used Ru as a metallic active phase in the hydrogenation of benzene [7,8], *o*-xylene [5,9,10] and polycyclic hydrocarbons [4,6,11–14] to examine the influence of Ru quantity [4,6], Ru precursors [7], Ru incorporation method [10], catalyst pretreatment [7–10] and support type [4,9,13,14] on the physicochemical properties and catalytic performance in the absence or presence [5,6,13,14] of sulphur compounds.

Kotanigawa et al. [4] have found that a catalyst with 0.1 wt.% Ru supported on Mn_2O_3–NiO exhibits excellent activity in selective hydrogenation of polycyclic aromatics. According to Jacquin et al. [12], MCM-supported Ru catalysts provide 95% naphthalene conversion at atmospheric pressure and 200 °C. Eliche-Quesada et al. [6] have revealed that of the mesoporous silica based Ru, Os and Ru-Os catalysts with a 5 wt.% total metal content, those containing the highest amount of Ru, display excellent hydrogenating properties in tetralin hydroconversion and a good thiotolerance to 600 ppm of DBT. In their further research they have found [13] that the activity and thiotolerance of 5 wt.% Ru catalysts increases with the acidity of the support. Tian et al. [14] have also observed the same support acidity effect.

E-mail address: Aleksandra.Masalska@pwr.wroc.pl.

0920-5861/$ – see front matter © 2008 Elsevier B.V. All rights reserved.
doi:10.1016/j.cattod.2008.01.009

In our previous studies on toluene hydrogenation [15,16] Ru was found to be a highly active promoter of Ni catalysts. Over a 0.15 wt.% Ru and 6.3 wt.% Ni (ZSM-5 + Al_2O_3) catalyst, toluene conversion exceeded 95% at 160–280 °C as compared to the 10–60% conversion at 240–280 °C over Ni catalysts. Some researches suggest that the second metal as a promoter affects catalytic performance in different ways. It can produce hydrogen spillover [17], enhance the reduction of the main metal and its dispersion [18], prevent the formation of carbonaceous deposits, and induce a cluster or ligand effect [19].

In this work use was made of Al_2O_3 + ZSM-5-supported 8 wt.% NiO catalysts displaying a high activity in selective hydrocracking of *n*-paraffin hydrocarbons [20,21]. The aim was to examine how the modification with Ru (0.6–0.9 wt.% of RuO_2) and the method of Ni catalyst preparation influence the activity of the dewaxing catalysts for the hydroconversion of the hydroraffinate of the oil fraction (HON) containing 25 ppm of S and 25.8 wt.% of aromatics.

2. Experimental

2.1. Catalyst preparation

The Ni catalysts (8 wt.% NiO) studied contained alumina and Ni,H-ZSM-5 zeolite (molar SiO_2/Al_2O_3 ratio of 35:1) at a 1:1 weight ratio (Table 1). They differed in the method of combining alumina and zeolite and the method of Ni incorporation. The preparation of series A catalysts involved 4 h aging of a mixture of zeolite and alumina hydrogel. The catalyst referred to as E was obtained by mixing two pastes: one containing ZSM-5 zeolite and 1% HNO_3, and the other one aluminium hydroxide and acid solution of nickel nitrate. As for the catalysts of series A and catalyst E, nickel was incorporated in a two-step procedure: one half during support formation, and the other half during impregnation (method F + I). As for the catalyst E_1, the whole amount of Ni was added at the stage of support formation (method F). Ru catalysts were obtained by impregnation of the Ni catalysts with an alcohol solution of Ru(III)acetyloacetonate. The catalysts were dried and calcined at 480 °C (for 3 h).

2.2. Catalyst characterisation

2.2.1. Porous structure

N_2 adsorption was measured at 77 K, using a Quantachrome Autosorb Automated Gas Sorption System. Prior to measurements, the sample was outgased under vacuum at 150 °C for 1 h.

2.2.2. Acidity

Acidity was analysed by chemisorption of ammonia at 180 °C in a through-flow system with a katharometer as a detector. More details are in a previous paper [15].

2.2.3. Chemical analysis

Ni and Ru content was determined by inductively Coupled Plasma-Atomic Emission Spectrometry (ICP-AES PU 7000 from Philips, Cambridge, UK) connected with an ultrasonic nebuliser CETAC (USA).

2.2.4. H_2 chemisorption

The volume of the H_2 adsorbed was measured at 35 °C with Micromeritics ASAP 2010C. The samples were reduced in a stream of H_2 at 500 °C (3 h). The Ni-Ru system was characterised only in terms of the volume of the H_2 adsorbed as in this bimetallic system adsorption temperature differs from one metal to another.

2.2.5. TPR experiments

Use was made of an Altamira AMI-1 system. The TPR of the catalyst was performed up to 850 °C, using a mixture containing

Table 1
Physicochemical properties of the catalysts

Catalyst code*	Metal content (wt.%)				RuO_2/Ru^0 crystallite size[a] (nm)	V[b] (cm^3/g)	Surface area) (m^2/g)		Pore volume (cm^3/g)		BJH pore diameter (nm)	Acidity (mmol NH_3/g)
	NiO		RuO_2				S_{BET}	St[c]	V_{total}[d]	V_{MIK}[c]		
	Nominal	Actual[e]	Nominal	Actual[e]								
A-8/0	8	8.3	0	–	–	0.404	269	233	0.35	0.039	5.6	0.82
A-12/0	12	11.5	0	–	–	0.730	215	127	0.31	0.037	5.7	0.84
A-0/0.6	0	–	0.6	0.57		–	278	207	0.35	0.041	5.8	0.81
A-8/0.6	8	7.8	0.6	0.58	52.6/–	–	256	181	0.36	0.035	6.4	0.78
A-8/0.75	8	7.7	0.75	0.76	43.6/–	–	262	187	0.32	0.034	6.4	0.75
A-8/0.9	8	7.8	0.9	0.85	42.1/11.6	0.689	266	190	0.35	0.035	6.5	0.74
E_1-8/0.9	8	8.1	0.9	0.89	45.7/17-23.8	0.599	231	183	0.29	0.025	5.2	0.82
E-8/0.9	8	7.8	0.9	0.87	42.0/13.8	0.623	261	186	0.34	0.035	5.6	0.77

Note: *Catalyst code M – *x*/*y*; where M is the method of alumina and zeolite combining; *x* and *y* stand for the amount (nominal) of NiO and RuO_2.
[a] The mean particle size of RuO_2/Ru^0 from XRD (before/after reduction at 500 °C for 3 h).
[b] The volume of hydrogen adsorbed.
[c] Calculated from *t*-plot.
[d] Calculated at relative pressure $p/p_0 = 0.99$.
[e] As determined by plasma emission spectroscopy.

80 vol.% of Ar and 20 vol.% of H_2 (>99.999%); gas velocity and heating rate being 40 cm^3/min and 15°/min, respectively.

2.2.6. XRD examinations

XRD patterns were obtained using a PANalytical X'Pert ProMPD diffractometer with a PW3050/65 high resolution goniometer, and operated at 40 kV and 30 mA (Cu Kα). Data were collected in the 2θ range 5–90° with step size of 0.0167 and 25.8 s time per step. The diffractograms were compared with the one taken from the JCPDX index. Mean crystallite size of Ru^0 and RuO_2 was calculated with Scherrer's method [22].

2.2.7. Scanning electron microscopy

Observations were performed using a Jeol JSM 5888 LV electron microscope with an Oxford Isis system for micro-analysis. Micrographs were obtained at 20 kV. The Ni and Ru distributions for NiKα and RuLα lines were determined.

2.2.8. X-ray photoelectron spectroscopy

XPS measurements were conducted using a SPECS PHOIBOS 100 spectrometer with an Mg Kα radiation. The spectrometer was calibrated with the Au $4f_{7/2}$, Ag $3d_{5/2}$ and Cu $2p_{3/2}$ lines at 84.2, 367.9 and 932.4 eV, respectively. The C 1s line (at 284.6 eV) was used as a reference. A nonlinear least-square fitting algorithm was applied using peaks with a mix of Gaussian and Lorentzian shape and a Shirley baseline. In the fitting of the Ni 2p profiles the FWHM values of the given sample were constant for all nickel species (Ni, NiO and Ni aluminate species).

2.2.9. Catalytic experiments

Catalytic activity was tested using the hydroraffinate of the oil fraction (HON) ($d_{20\,°C}$ = 0.845 g/cm^3; cloud point (CP) = −2 °C; cold filter plugging point (CFPP) = −6 °C; S = 25 ppm; aromatics = 25.8 wt.%; C_A = 16.9%) in a continuous-flow system with a fixed-bed reactor at H_2 pressure of 6 MPa (LHSV = 2.5 h^{-1} and H_2:CH = 350 N m^3/m^3). The catalyst (4 cm^3, 0.50–0.75 mm) was activated in H_2 flow at a heating rate of 10°/min up to 300 °C (1 h) and 480 °C (1 h). Liquid products were condensed at the reactor outlet, typically accumulated for 1 h, weighed and analysed. Carbon content in the aromatic structure (C_A by IR at 1610 cm^{-1} [23]) and aromatics content by HPLC were taken as a measure of the catalyst hydrogenating properties; the measure of dewaxing activity being the cloud point of the products and the cold filter plugging point.

3. Results and discussion

3.1. Effect of ruthenium content

The chemical composition of the catalysts shows that the content of metals is close to the nominal one, and irrespective of metal loading, all catalysts display a similar texture (Table 1). NH_3 chemisorption results indicate that the incorporation of RuO_2 and further rise in RuO_2 content up to 0.9 wt.% reduces surface acidity of nickel catalyst from 0.82 to 0.74 mmol/g (seemingly, RuO_2 has covered the acid sites with metal clusters).

The XRD diffractograms of catalysts (not shown) did not significantly differ in the morphology. The XRD patterns revealed a splitting of the strongest line at 23.10 2θ, which is characteristic for the Ni-form of the ZSM-5 zeolite. None of the catalysts tested showed characteristic X-ray diffraction lines for NiO and $NiAl_2O_4$, probably because of a poor crystallinity. RuO_2 crystallites were found to occur in Ru-modified Ni catalysts. Calculated on the basis of the peak positions at 2θ around 28.2° and 35.2°, the crystallite size for catalysts containing 0.6, 0.75 and 0.9 wt.% of RuO_2 amounted to 52.6, 43.6 and 42.1 nm, respectively.

The TPR results (Fig. 1) disclose a low reducibility of Ni species for the Ni catalysts (A-8/0 and A-12/0). The TPR profiles of these catalysts display small peaks at 350–500 °C and broad main reduction peaks at 550–850 °C with shoulders located at ca. 650 °C, one of these being particularly distinct for A-12/0. Even at 850 °C not all the Ni atoms are reduced. The low reducibility of the Ni^{2+} is linked with strong interactions between Ni oxide species and alumina. Such interactions (resulting in surface Ni–Al oxide spinels) have been reported by many authors [24–26]. There are references in the literature [18,27] to spinels of Ni–Al oxides that reduce at temperatures higher than 700 °C while an amorphous overlayer of NiO, which is not chemically bound, interacts less or more with the support below 500 °C and within 550–700 °C, respectively. The modification of Ni catalyst (A-8/0) with 0.6 wt.% of RuO_2 (A-8/0.6) noticeably increases the reducibility of oxidic Ni species. There is an increase in the proportion of NiO which reduces at 250–700 °C, and an almost complete reduction of Ni^{2+} at 850 °C. Additionally, a shift of the low-temperature peak (from

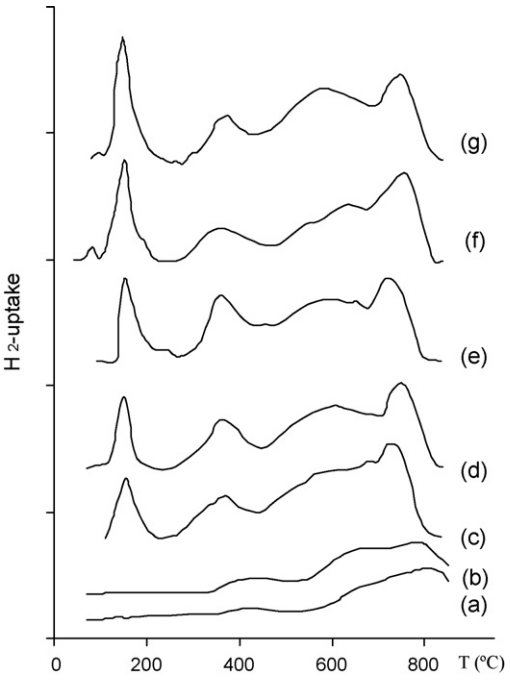

Fig. 1. TPR profiles of catalysts: (a) A-8/0; (b) A-12/0; (c) A-8/0.6; (d) A-8/0.75; (e) A-8/0.9; (f) E_1-8/0.9; (g) E-8/0.9.

420 to 380 °C) and of the shoulder (from 650 to 550 °C) is observed for A-8/0.6 (as compared to A-8/0). When the amount of RuO_2 rises from 0.6 to 0.9 wt.%, this is parallelled by a further increase in the reducibility of the NiO phase: the proportion of NiO that reduces at 250–450 °C increases from 15 to 21%, and that of Ni oxide species which reduces above 700 °C decreases from 29 to 23%. The occurrence of the peak at ca. 150 °C is linked with RuO_2 reduction [18].

The catalytic activities of the investigated catalysts are plotted in Fig. 2. The results have revealed that, over the 8 wt.% NiO catalyst (A-8/0) and the 0.6 wt.% RuO_2 catalyst (A-0/0.6), the decrease in the CP of the products to −20 °C required reaction temperature above 240 °C (Fig. 2a). At these temperatures, the catalysts showed no activity in the hydrogenation of aromatics but displayed dehydrogenating properties (Fig. 2b). In comparison with the catalysts that contain NiO or RuO_2 alone, the catalyst which includes both the active metals (A-8/0.6) showed an enhanced activity, which is attributable to the synergic effect of the two metals. At 240 °C there was a satisfactory drop in CP (ca. 18 °C) parallelled by the HDA (calculated on the basis of C_A drop) of HON that equalled 23%. The rise in the catalytic activity of the Ru-modified Ni catalyst is due not only to the presence of Ru, which has a higher hydrogenating activity than Ni, but also to the Ru-Ni interaction, which raises the reducibility of NiO. It seems that the favoured NiO reduction is caused by the fact that RuO_2 is reduced first, thus activating hydrogen and evoking the spillover effect [17]. The promoting effect of Ru on the reduction of the oxidic Ni phase at a low doping content has also been reported [18]. The modification of the metal function of the 8 wt.% NiO catalyst with 0.6 wt.% of RuO_2 yielded a catalyst (A-8/0.6) with a higher activity as compared to that modified by additional incorporation of 4 wt.% NiO (A-12/0) (Fig. 2).

The rise in RuO_2 content from 0.6 to 0.9 wt.% decreases the CP of the products (Fig. 2a), which is particularly distinct at 240 °C (by about 15 °C). There is also a decrease in the carbon content in the aromatic structures (C_A by IR) (Fig. 2b). Thus, the increase in RuO_2 content over the range mentioned increases the HDA of HON (calculated from the drop in C_A) from 53 to 82% (by 29%) at 200 °C and from 23 to 65% (by 42%) at 240 °C. The enhancement of hydrogenating properties is attributable not only to the increased RuO_2 content but also to the further increased reducibility of the Ni oxide species.

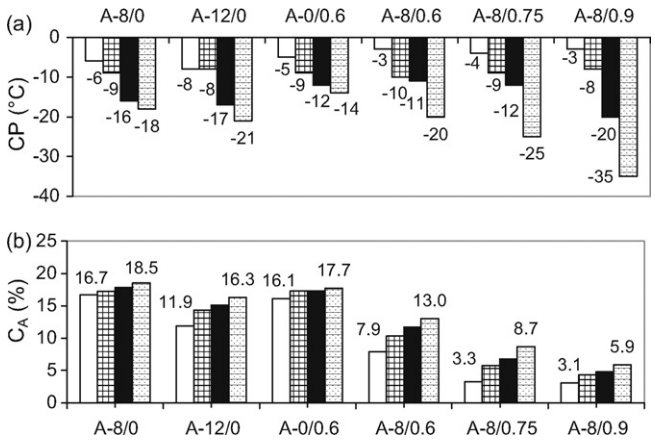

Fig. 2. Effect of Ru amount on (a) cloud point of products (CP) and (b) aromatics content (C_A) at reaction temperature of 200 °C (□), 220 °C (▦), 230 °C (■) and 240 °C (⊡).

3.2. Method of nickel catalyst preparation

The occurrence of a synergic effect between NiO and RuO_2 has directed our attention to the problem of how the method of Ni catalyst preparation influences the activity of the Ru-modified Ni catalysts. Thus, 0.9 wt.% of RuO_2 was incorporated into the catalysts that differed not only in the method of combining alumina and zeolite (methods A and E) but also in the method of Ni incorporation (methods F + I and F). As can be seen in Table 1, A-8/0.9 and E-8/0.9 display a comparable texture even though the mean pore diameter of A-8/0.9 is slightly higher. Compared with the two catalysts mentioned, the BET area (231 mm^2/g), the pore volume (0.29 cm^3/g) and the mean pore diameter (5.2 nm) of E_1-8/0.9 are the lowest. Chemisorption measurements via ammonia have shown that acidity is the highest for E_1-8/0.9 (0.82 mmol/g) as compared to E-8/0.9 and A-8/0.9 (0.77 and 0.74 mmol/g, respectively).

The XRD results for the catalysts after reduction for 3 h at 500 °C (not shown) were similar. There are no characteristic diffraction lines either for Ni and NiO or for $NiAl_2O_4$ but there are diffraction lines for Ru^0 crystallites. The size of Ru^0 crystallites (calculated from the peak positions at 2θ around 38.4° and 44.0°) is the smallest (11.6 nm) for A-8/0.9 compared to E-8/0.9 and E_1-8/0.9 (13.8 and 17.0–23.8 nm, respectively). The XRD results are consistent with those of H_2 chemisorption. The volume of the H_2 adsorbed can be ordered as follows: E_1-9/0.9 < E-9/0.9 < A-9/0.9 (Table 1).

Ru and Ni distribution on the catalyst surfaces detected by SEM is depicted in Fig. 3. As shown by these micrographs, Ni distribution across the surface of A-8/0.9 is slightly more uniform compared to E-8/0.9 and E_1-8/0.9. The comparison of the dot mappings for Si (indicating the presence of zeolite crystals) makes it clear that in E-8/0.9 and E_1-8/0.9 nickel is deposited mainly on alumina. The SEM micrographs of Ru have revealed that the catalysts tested display smaller (A-8/0.9) or larger (E_1-8/0.9) Ru aggregates.

The TPR results show (Fig. 1) that the method of Ni catalyst preparation influences the reducibility of the Ru-modified Ni catalysts. When in the preparation of E_1-8/0.9 (Fig. 1f) the whole NiO amount (8 wt.%) was added during formation of the paste of aluminium hydroxide and nickel nitrate (method F), the proportion of NiO which reduces above 700 °C (Ni^{2+} in spinel structure) is the highest (ca. 35%) as compared to A-6/0.9 (ca. 23%) and E-6/0.9 (ca. 25%). Such procedure induces a strong interaction between Ni and alumina and favours the formation of species that are more difficult to reduce. Compared to E_1-6/0.9, the TPR pattern for E-8/0.9 (Fig. 1g) shows a rise in the proportion of NiO reducible at 450–700 °C (by ca. 14%), as only half of the Ni portion was added during support formation. Reducibility was found to be the highest for A-8/0.9 (Fig. 1e). The profile of this catalyst displays the highest proportion of NiO that reduces at 275–450 °C (ca. 21%) as compared to E_1-6/0.9 and E-6/0.9 (ca. 15 %). In A-8/0.9 preparation, Ni was also

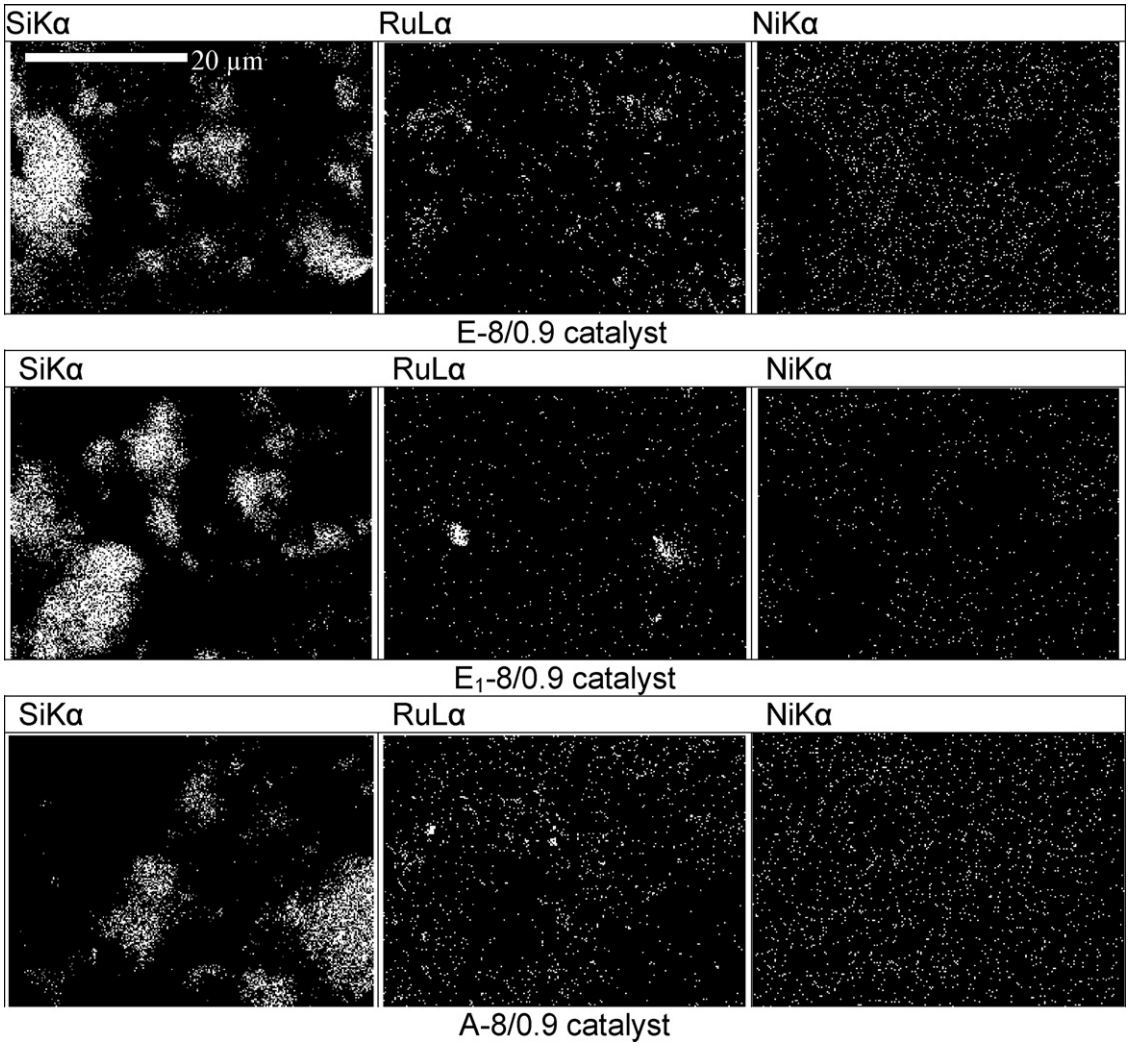

Fig. 3. SEM micrographs of the catalysts: distribution of silica, ruthenium and nickel on the surface of the catalysts.

incorporated by a method F + I but in contrast to E-8/0.9 (the Ni portion added only into alumina), the Ni portion was added into the mixture of zeolite and alumina; therefore, the interaction between alumina and Ni was the lowest. The TPR patterns of the catalysts imply that NiO and RuO_2 occur separately on the catalyst surface (peak at about 150 °C in the RuO_2 reduction region). However, the smallest proportion below the RuO_2 reduction peak for A-8/0.9 (lower hydrogen uptake) indicates that the largest amount of residual RuO_2 is in an intimate contact with NiO. Seemingly, A-8/0.9 contains a larger quantity of bimetallic NiRu oxide clusters (easier reducible than those of NiO) than do E-8/0.9 and E_1-8/0.9. The formation of Ni-Ru clusters is reported in the literature [17,18,28].

The XPS method was used to determine the chemical state of the surface species in Ni-Ru catalysts. The binding energy (BE) of Ru $3d_{5/2}$ was chosen to estimate the relative amounts of the Ru species that were present on the surface because the carbon peak (284.5 eV) overlaps the Ru $3d_{3/2}$ region. The BE of Ru $3p_{3/2}$ could not be considered as the 461–464 eV region was overlapped by impurities difficult to identify. According to literature, the signals at BE (Ru $3d_{5/2}$) for 279.6–279.9 eV, at ca. 280.7 eV, and for 282.5–283.0 eV can be assigned to Ru^0, RuO_2 and RuO_3, respectively [29,30]. Only weak signals were detected on the XPS spectra of the Ru $3d_{5/2}$ region (not shown), because the amount of Ru on the catalyst surfaces was very low (0.08–0.1 at.%). To evaluate the relative amount of Ni species on the catalyst surface, the Ni $2p_{3/2}$ region of the XPS spectra was taken into account. The BE data for Ni species obtained following deconvolution are summarised in Table 2 and plotted in Fig. 4. The XPS spectra show peaks at BE 853.1 and 855.6 eV corresponding closely to the values reported for metallic Ni (853.0 eV [31]) and NiO (854.0–855.0 eV [31,33]). The presence of metallic Ni and stoichiometric NiO at BE showing values slightly higher than 853.0 and the 855.0 eV (characteristic for pure Ni and NiO) suggests weak interactions with the support. According to literature [31–34], the signals at higher BE (856.5–857.2 eV) can be assigned to Ni aluminate species. As can be seen from Fig. 4 and Table 2, the relative amount of Ni^0 in A-8/0.9 is higher than in E-8/0.9 and E_1-8/0.9. The results of XPS and TPR are consistent.

The differences in reducibility between the Ru-modified Ni catalysts manifest in their activity (Table 2). The comparison of the aromatics content with the cold-flow properties of the products (stabilised samples, after 10 h on stream) shows that the

Table 2
Effect of Ni catalyst preparation on XPS data and the activity of Ru-Ni catalysts in HON hydroconversion (T = 240 °C; LHSV = 2.5 h^{-1}; H_2:CH = 350 N m^3/m^3)

Catalyst	BE (eV) of Ni $2p_{3/2}$ levels after deconvolution				Activity of catalysts**							
	FWHM (eV)	Ni	NiO	$NiAlO_4$	Cold-flow properties (°C)		Aromatics content by IR at 1610 cm^{-1}		Aromatics content by HPLC (wt.%)			
					CP	CFPP	C_A (%)	HDA (%)	M	Di	Di^+	T	HDA (%)
Feed	–	–	–	–	−2	−6	16.9	–	22.8	2.6	0.4	25.8	–
A-8/0.9	4.30	853.1 (17%)*	855.6 (71%)	857.2 (12%)	−22	−24	6.9	59.2	11.6	0.1	0.1	11.8	54.3
E_1-8/0.9	4.38	853.1 (8%)	855.6 (76%)	857.2 (16%)	−19	−22	13.6	19.5	21.0	0.6	0.1	21.7	15.9
E-8/0.9	3.69	853.1 (11%)	855.6 (79%)	857.2 (10%)	−18	−22	10.7	36.7	16.9	0.4	0.1	17.4	32.6

Note: *Proportion of surface beneath relevant peak; **products accumulated for 10 h on stream; CP, cloud point; CFPP, cold filter plugging point; C_A, carbon content in the aromatic structure; HDA, hydrodearomatisation; M, monoaromatics; Di, diaromatics; Di^+, polyaromatis; T, total.

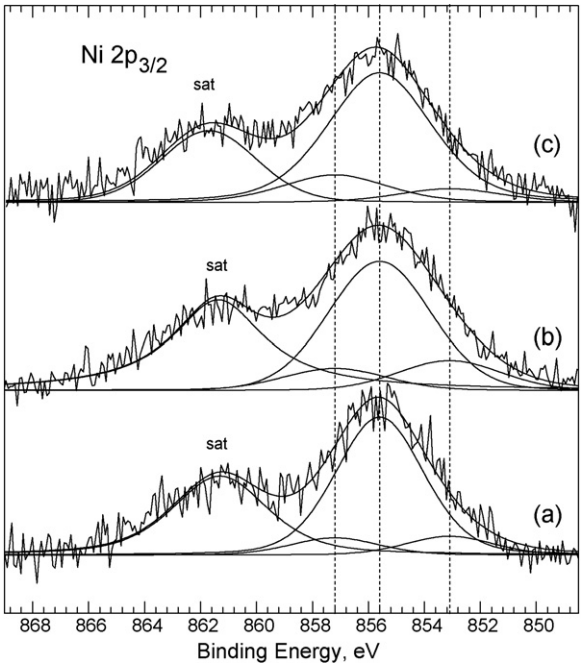

Fig. 4. XPS spectra of Ni $3p_{3/2}$ region for catalysts: (a) E-8/0.9; (b) A-8/0.9; (c) E_1-8/0.9.

preparation procedure enhanced the catalytic properties of A-8/0.9 with respect to aromatics hydrogenation and increased its hydrocracking activity (HDA above 50 %, CP = −22° and CFPP = −24 °C at 240 °C). This enhancement is due to the increased reducibility of Ni species, the increased dispersion of Ni and Ru (higher H_2 adsorption, smaller Ru crystallites revealed by XRD) as well as more uniform distribution of metals (SEM). It is worth noticing that for all investigated catalysts the loss in the carbon balance (the low molecular weight products and tar deposits) is low (below 2.8 wt.% at 240 °C).

4. Conclusions

The research onto the modification of Ni-based dewaxing catalysts with Ru for the hydroconversion of HON enabled the following conclusions to be drawn:

1. Compared to the catalysts containing NiO or RuO_2 alone, the catalyst containing both active metals shows an enhanced activity attributable to the synergic effect of the two metals.
2. At 240 °C, the increase in RuO_2 content from 0.6 to 0.9 wt.% accounted for a 42% increase in HDA of HON and a satisfactory drop in the CP of the products. Such enhancement in catalytic activity is attributable not only to the increased Ru content but also to the parallel increase in the reducibility of the Ni species.
3. The effect of Ru was found to depend on the method of Ni catalyst preparation. When Ni was incorporated into the zeolite and alumina hydrogel mixture, the activity of the catalyst with respect to aromatics hydrogenation, as well as its dewaxing activity, was high, which is due to the high reducibility of the NiO phase and the increased dispersion of Ru and Ni.

Acknowledgement

The financial support by Ministry of Education and Science is gratefully acknowledged (N205 066 31/3012).

References

[1] World-wide Fuel Charter, fourth ed., September 2006.
[2] B.H. Cooper, B.B.L. Donnis, Appl. Catal. A: Gen. 137 (1996) 203.
[3] I. Skręt, Bull. Inst. Petrol. Process. XII/4 (2000) 296, ISSN 1233-3867.
[4] T. Kotanigawa, M. Yamamoto, T. Yoshida, Appl. Catal. A: Gen. 164 (1997) 323.
[5] A. Arcoya, X.L. Seoane, L.M. Gómez-Sainero, Appl. Surf. Sci. 211 (2003) 341.
[6] D. Eliche-Quesada, J.M. Mérida-Robles, E. Rodríguez-Castellón, A. Jiménez-López, Appl. Catal. A: Gen. 279 (2005) 209.
[7] C. Milone, G. Neri, A. Donato, M.G. Musolino, L. Mercadante, J. Catal. 159 (1996) 253.
[8] V. Mazziere, F. Coloma-Pascual, A. Arcoya, P.C. L'Argentiére, N.S. Fígoli, Appl. Surf. Sci. 210 (2003) 222.
[9] P. Reyes, M.E. König, G. Pecchi, I. Concha, M. Lopez Granados, J.L.G. Fierro, Catal. Lett. 46 (1997) 71.
[10] T. Lopez, P. Bosch, M. Asomoza, R. Gomez, J. Catal. 133 (1992) 247.
[11] S. Albertazzi, R. Ganzerla, C. Gobbi, M. Lenarda, M. Mandreoli, E. Salatelli, P. Savini, L. Storaro, A. Vaccari, J. Mol. Catal. A: Chem. 200 (2003) 261.
[12] M. Jacquin, D.J. Jones, J. Rozière, S. Albertazzi, A. Vaccari, M. Lenarda, L. Storaro, R. Ganzerla, Appl. Catal. A: Gen. 251 (2003) 131.
[13] D. Eliche-Quesada, M.I. Macías-Ortiz, J. Jiménez-Jiménez, E. Rodríguez-Castellón, A. Jiménez-López, J. Mol. Catal. A: Chem. 225 (2006) 41.
[14] P. Tian, J. Blanchard, K. Fajerwerg, M. Breysse, M. Vrinat, Z. Liu, Microporous Mesoporous Mater. 60 (2003) 197.
[15] A. Masalska, Appl. Catal. A: Gen. 294 (2005) 260.
[16] A. Masalska, Pol. J. Environ. Stud. 14 (2005) 247.
[17] C. Crisafulli, S. Scire, S. Minico, L. Solarino, Appl. Catal. A: Gen. 225 (2002) 1.
[18] J.M. Rynkowski, T. Paryjczak, M. Lennik, Appl. Catal. A: Gen. 126 (1995) 257.
[19] G. Cordoba, J.L.G. Fierro, A. Lopez-Gaona, N. Martin, M. Viniegra, J. Mol. Catal. A: Chem. 96 (1995) 155.
[20] J.R. Grzechowiak, A. Masalska, J. Grzechowiak, Przemysł Chemiczny 75 (1996) 295.
[21] A. Masalska, Catal. Today 65 (2001) 271.
[22] H.P. Klug, L.E. Alexander, X-ray Diffraction Procedures, Wiley, New York, 1974, p. 661.
[23] R.A. Puszkina, A. Kuklinski, Neftechimia 3 (1980) 350.
[24] Ch. Li, Y.W. Chen, Thermochim. Acta 256 (1995) 457.
[25] J.T. Richardson, M.V. Twigg, Appl. Catal. A: Gen. 167 (1998) 57.
[26] A. Gil, A. Diaz, L.M. Gandia, M. Montes, Appl. Catal. A: Gen. 109 (1994) 167.
[27] J.M. Rynkowski, T. Paryjczak, M. Lennik, Appl. Catal. A: Gen. 106 (1993) 73.
[28] C. Crisafulli, S. Scire, R. Maggiore, S. Minico, S. Galvagno, Catal. Lett. 59 (1999) 21.
[29] M. Nagai, K. Koizumi, S. Omi, Catal. Today 35 (1997) 393.
[30] C.R. Lederhos, P.C. L'Argientiere, F. Coloma-Pascual, N.S. Figoli, Catal. Lett. 110 (2006) 23.
[31] P. Salagre, J.L.G. Fierro, F. Medina, J.E. Sueiras, J. Mol. Catal. A: Chem. 106 (1996) 125.
[32] T. Long-Xiang, Z. Feng-Mei, Z. Lu-Bin, React. Kinet. Catal. Lett. 57 (1996) 99.
[33] T.F. Petti, D. Tomczak, C.J. Pereira, W.Ch. Cheng, Appl. Catal. A: Gen. 169 (1998) 95.
[34] A.N. Kharat, P. Pendleton, A. Badalyan, M. Abedini, M.M. Amini, J. Catal. 205 (2002) 7.